Electronic Supplementary Information (ESI)

Cobalt(III) complexes with tridentate hydrazone ligands: protonation state and hydrogen bonds competition

Višnja Vrdoljak, Gordana Pavlović, Tomica Hrenar, Mirta Rubčić, Patrizia Siega, Renata Dreos and Marina Cindrić

Contents:

DSC thermograms

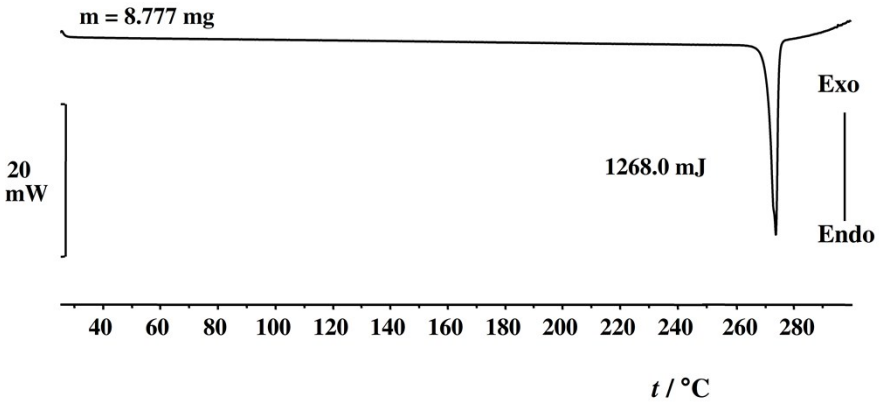

Fig. S1 DSC thermogram of H_2L^1

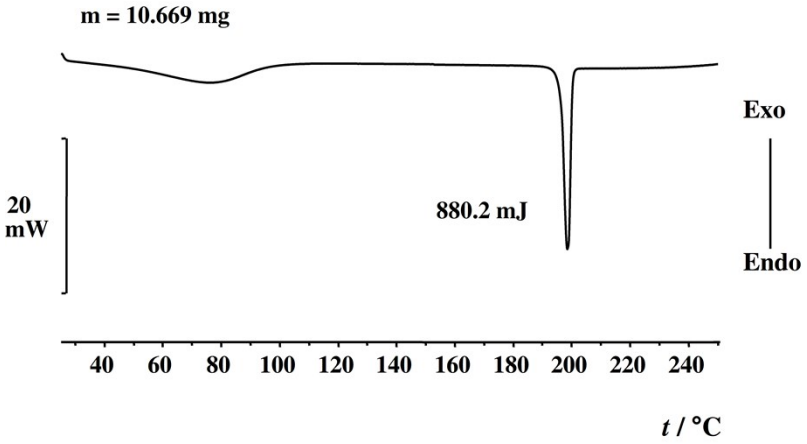

Fig. S2 DSC thermogram of $H_2L^2 \cdot H_2O$

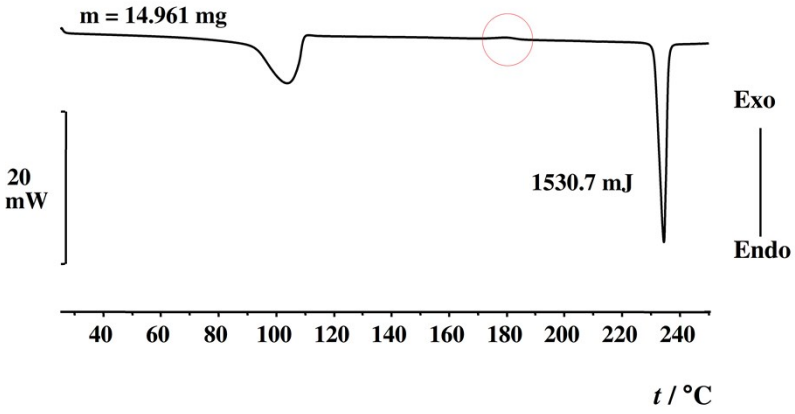

Fig. S3 DSC thermogram of $H_2L^3 \cdot H_2O$

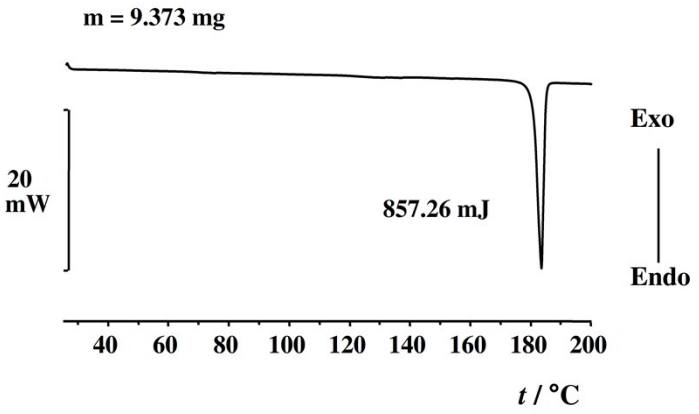

Fig. S4 DSC thermogram of H_2L^4

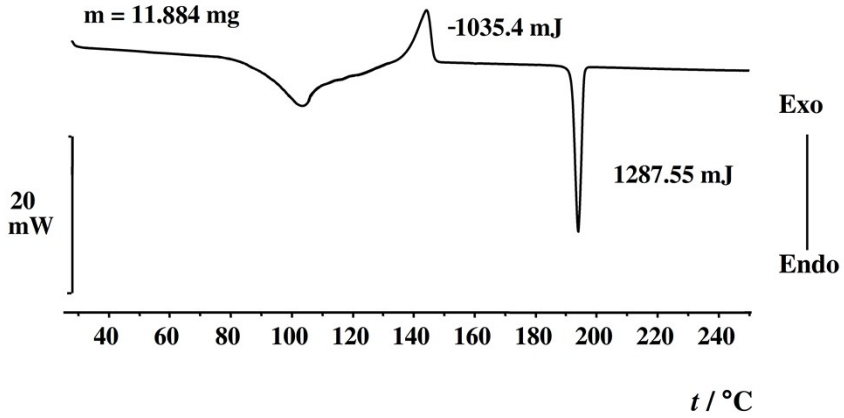

Fig. S5 DSC thermogram of $H_2L^5 \cdot H_2O$

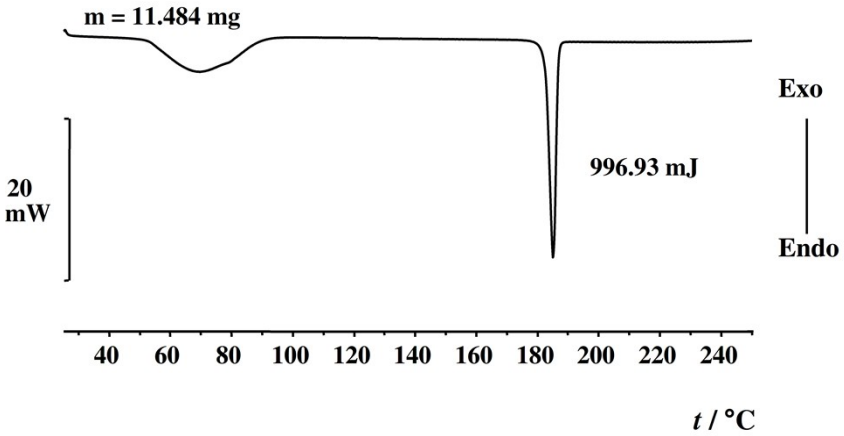

Fig. S6 DSC thermogram of $H_2L^6 \cdot H_2O$

Powder X-ray diffraction patterns

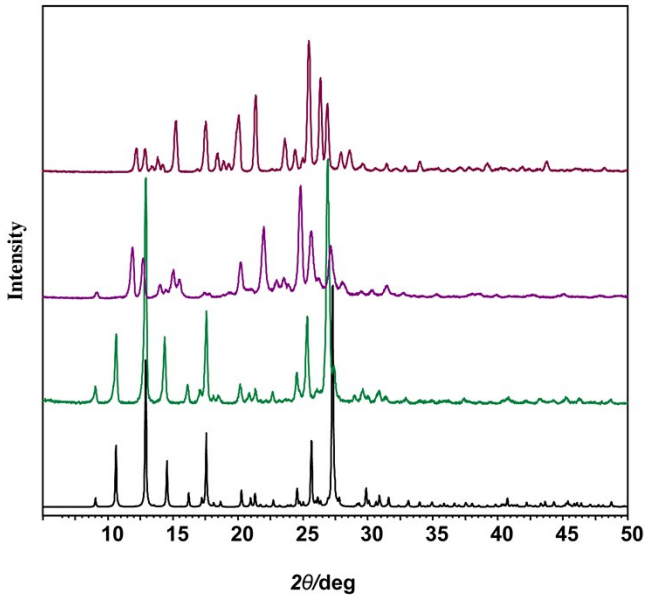

Fig. S7 PXRD patterns for $H_2L^3 \cdot H_2O$

(from top to bottom): of sample obtained when $H_2L^3 \cdot H_2O$ was heated from the ambient temperature up to 200 °C at 5 °C min^{-1}; of sample obtained when $H_2L^3 \cdot H_2O$ was heated from the ambient temperature up to 120 °C at 5 °C min^{-1}; of mechanochemically prepared $H_2L^3 \cdot H_2O$ ligand; and calculated from the deposited crystal structure (CSD code MOKRUA).

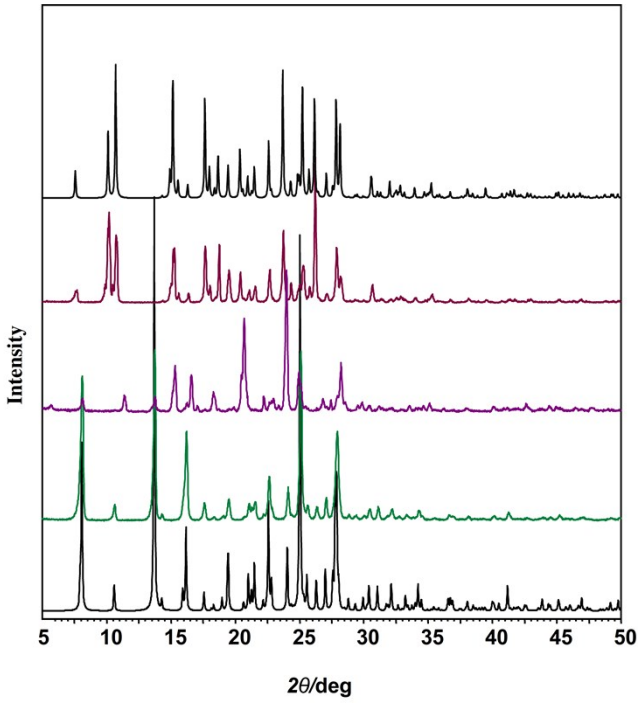

Fig. S8 PXRD patterns for $H_2L^5 \cdot H_2O$

(from top to bottom): of H_2L^5 calculated from the X-ray single-crystal structure; of sample obtained when $H_2L^5 \cdot H_2O$ was heated from the ambient temperature up to 150 °C at 5 °C min^{-1}; of sample obtained when $H_2L^5 \cdot H_2O$ was heated from the ambient temperature up to 125 °C at 5 °C min^{-1}; of mechanochemically prepared $H_2L^5 \cdot H_2O$ ligand; and calculated from the deposited crystal structure (CSD code TEZMER).

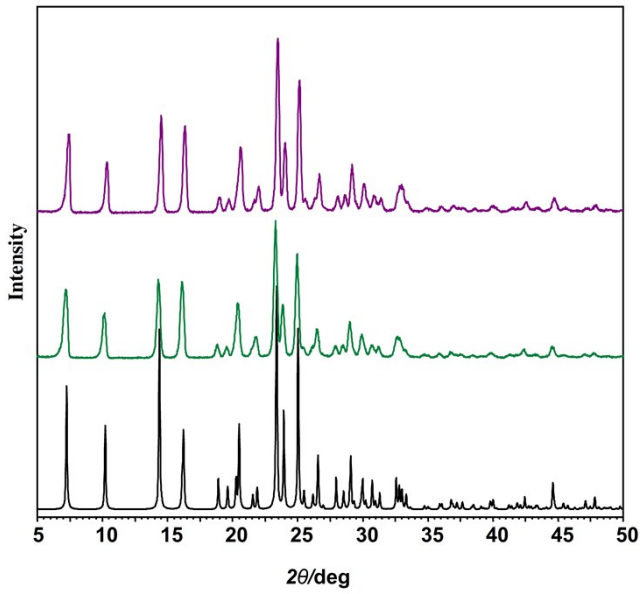

Fig. S9 PXRD patterns for $H_2L^2 \cdot H_2O$

(from top to bottom): of sample obtained when $H_2L^2 \cdot H_2O$ was heated from the ambient temperature up to 150 °C at 5 °C min^{-1}; of mechanochemically prepared $H_2L^2 \cdot H_2O$ ligand; and calculated from the deposited crystal structure (CSD code ROGFEZ).

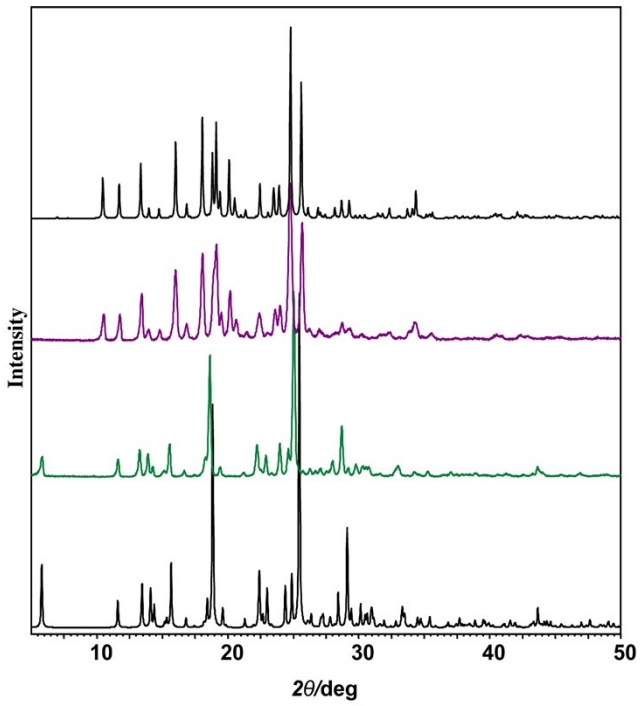

Fig. S10 PXRD patterns for $H_2L^6 \cdot H_2O$

(from top to bottom): of H_2L^5 calculated from the X-ray single-crystal structure of sample obtained when $H_2L^6 \cdot H_2O$ was heated from the ambient temperature up to 120 °C at 5 °C min^{-1}; of mechanochemically prepared $H_2L^6 \cdot H_2O$; and calculated from the deposited crystal structure (CSD code MIQXUH).

TG curves

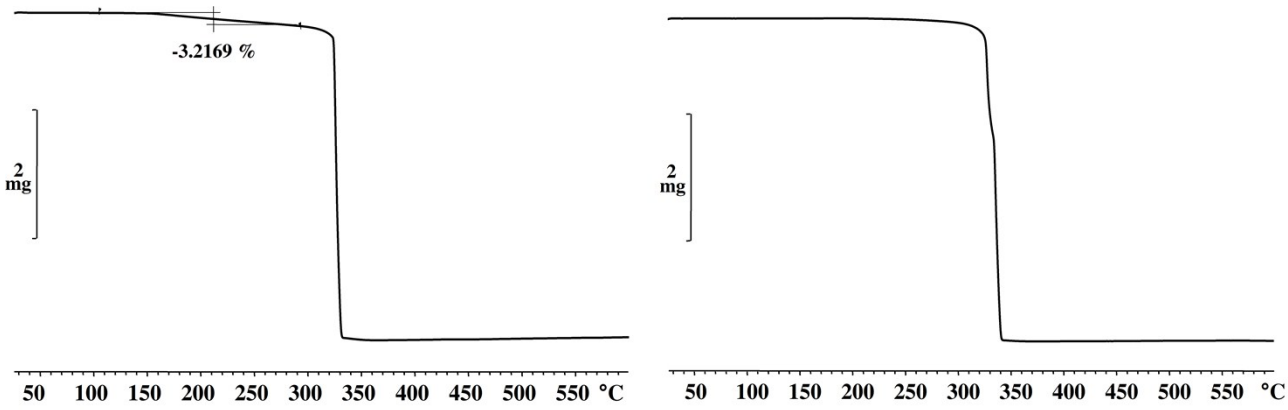

(a) (b)

Fig. S11 TG curves (a) of the crystalline sample **2·0.7CH$_3$OH**; and (b) of guest free sample obtained upon standing at room temperature affording **2**. Experiments were recorded with a heating rate of 5 °C min^{-1} in a dynamic atmosphere with a flow rate of 200 cm^3 min^{-1}.

Crystal and molecular structures

H_2L^3

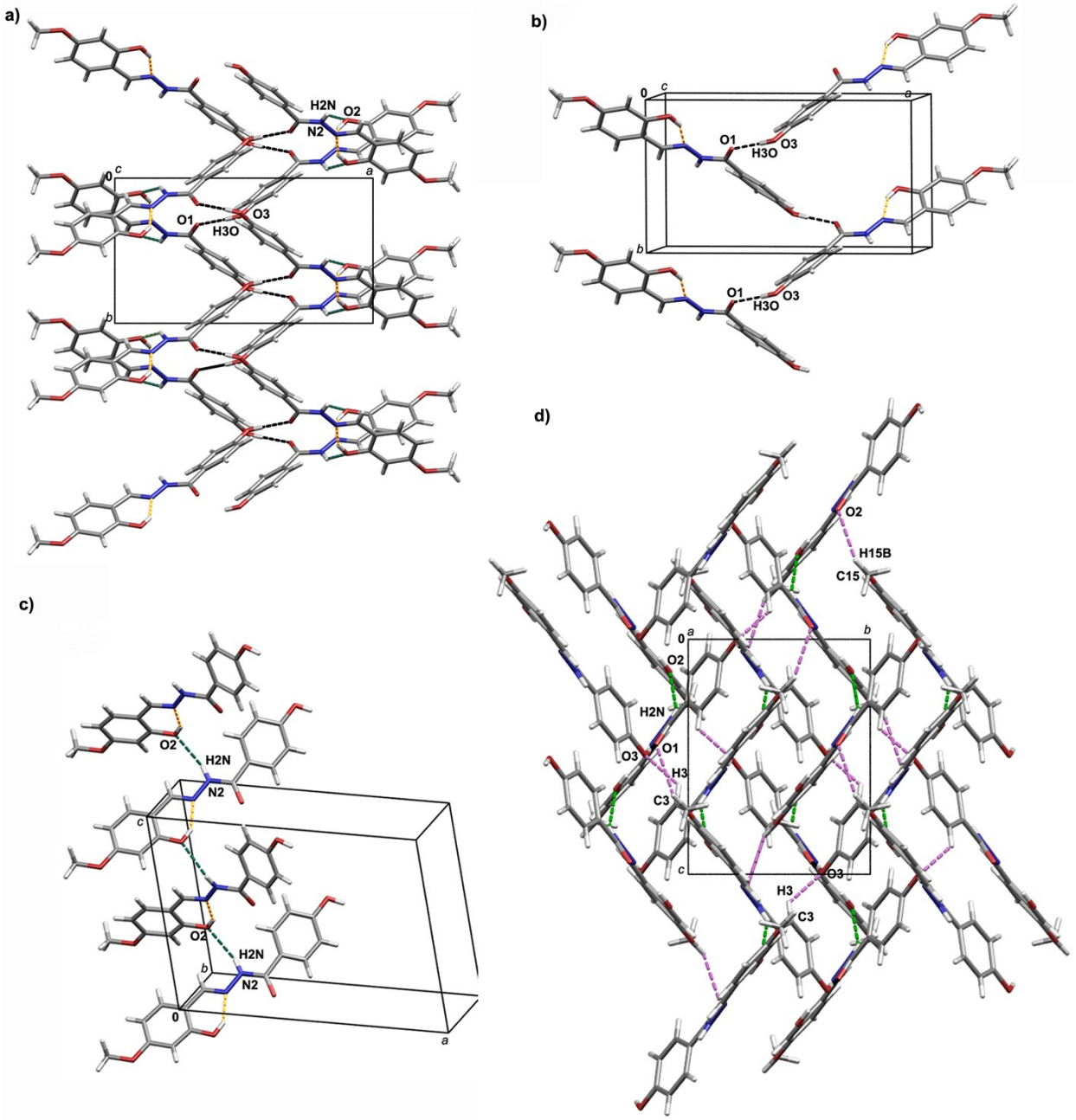

Fig. S12 a) View of the complex hydrogen-bonded network observed for H_2L^3 down the *c*-axis. The network is shaped by two types of intersecting hydrogen-bonded chains: b) the ones realized through O3–H3O···O1 hydrogen bonds (shown as black dashed lines) that run along the *b*-axis (*C*(8) motif), and c) those accomplished *via* N2–H2N···O2 hydrogen bonds (shown as green dashed lines) that grow along the *c*-axis (*C*(7) motif). Hydrogen-bonded network shown in a) is stabilized and expanded into a 3D architecture *via* C3–H3···O3 and C15–H15B···O1 interactions (shown as purple dashed lines), respectively. Intramolecular hydrogen bonds in a)–c) are illustrated by orange dashed lines.

H_2L^5

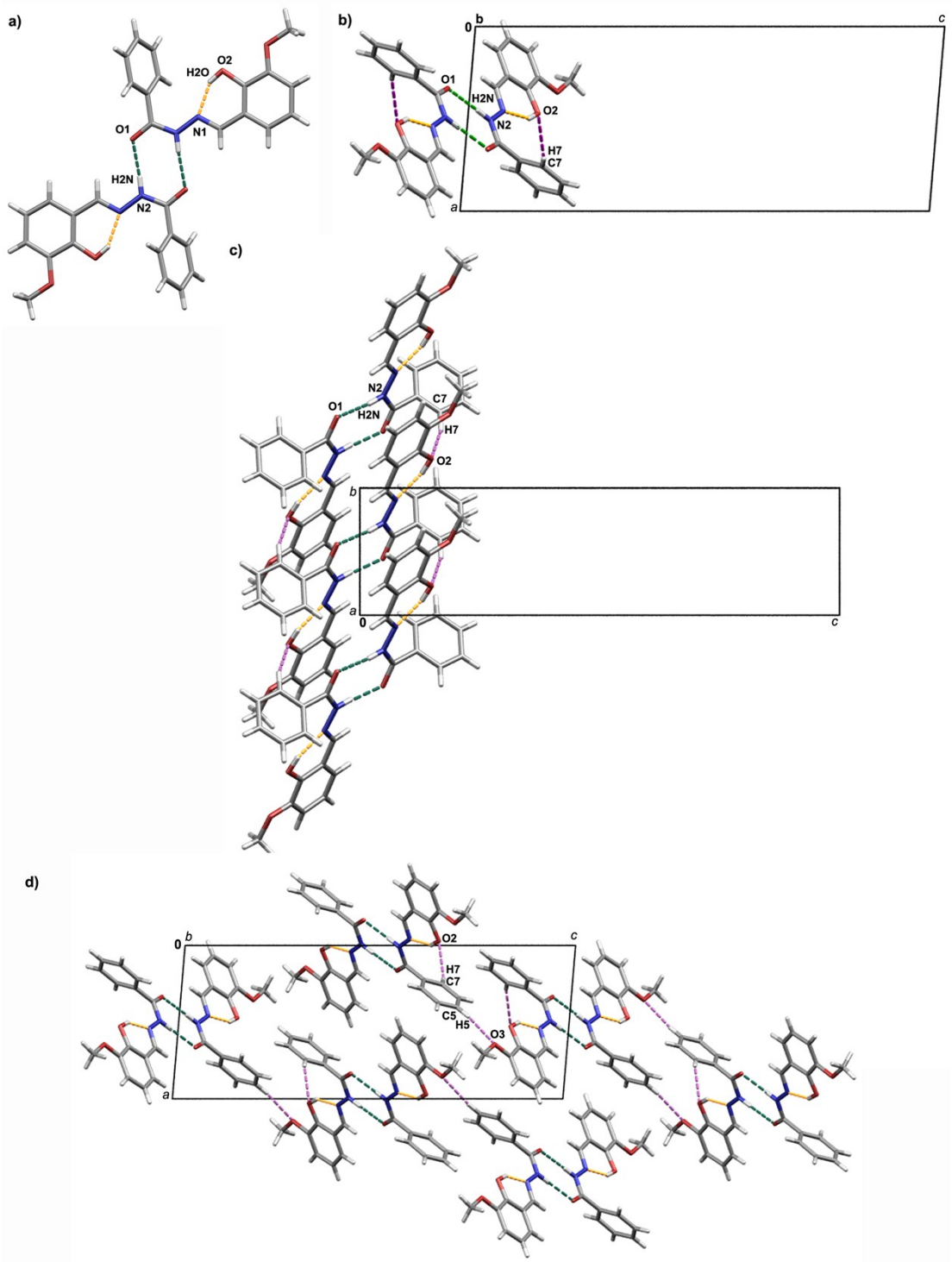

Fig. S13 a) Centrosymmetric hydrogen-bonded dimers displaying a $R_2^2(8)$ motif form *via* N2–H2N···O1 hydrogen bonds (shown as green dashed lines). The dimers associate through C7–H7···O2 interactions (shown as purple dashed lines) into endless chains which run along the *b*-axis. View of the chains along the *b*- and *a*-axis are shown in b) and c), respectively. d) Chains further assemble into layers *via* C5–H5···O3 interactions (shown as purple dashed lines) which are finally stacked through van der Waals interactions. In a)-d) intramolecular hydrogen bonds, O2–H2O···N1, are highlighted by orange dashed lines.

H_2L^6

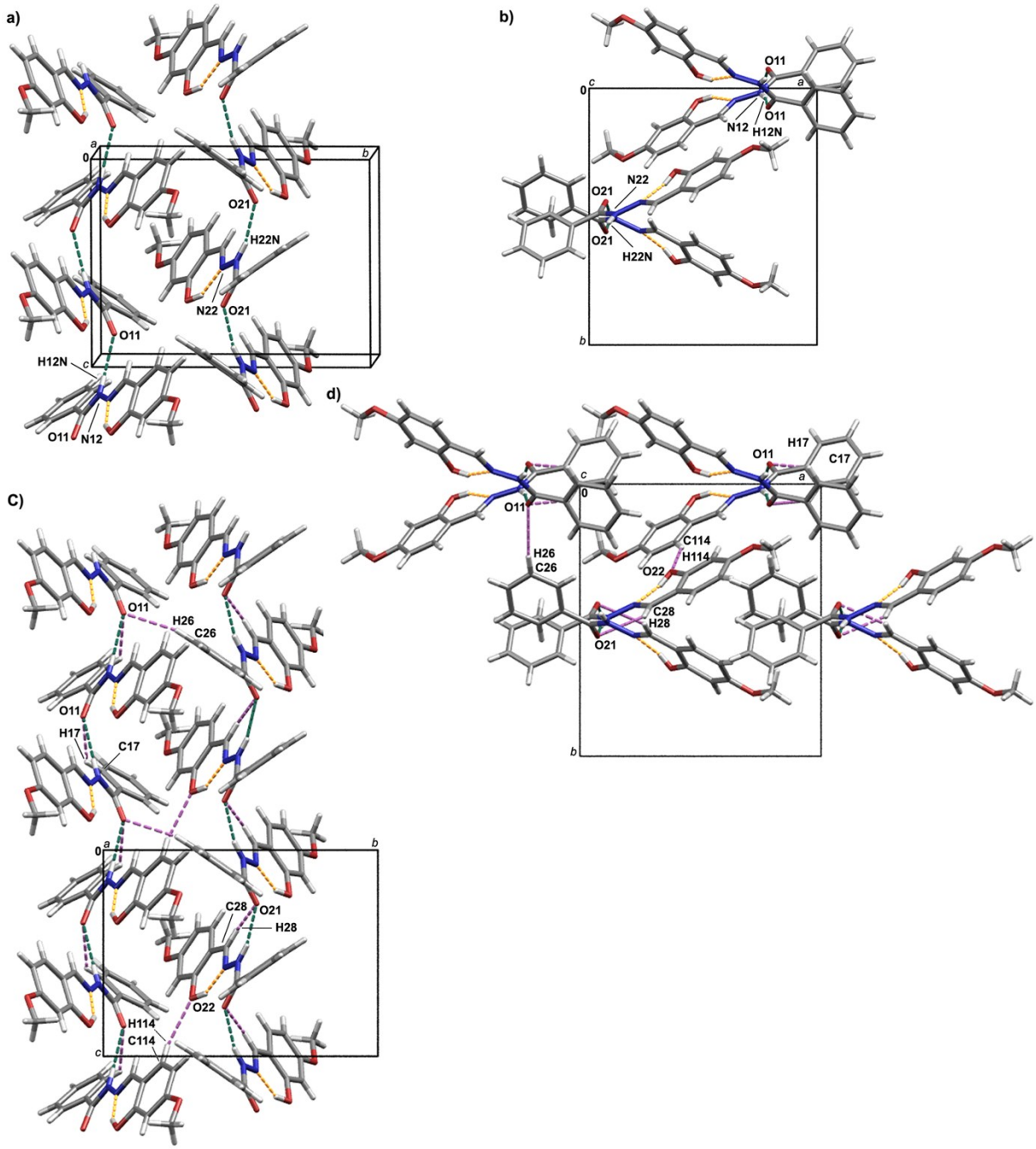

Fig. S14 a) Hydrogen bonded chains exhibiting a *C*(4) motif are realized through N12–H12N···O11 and N22–H22N···O21 hydrogen bonds (shown as green dashed lines) when considering molecules 1 and 2, respectively. b) Projection of the chains shown in a) along the *c*-axis. c) Supramolecular chain comprising molecules 1 is stabilized *via* C17–H17···O11 interactions, whereas the one comprising molecules 2 is stabilized through C28–H28···O21 interactions. Such chains are interconnected by C26–H26···O11 and C114–H114···O22 interactions. d) Projection of the network shown in c) along the *c*-axis. C–H···O interactions in c) and d) are shown as purple dashed lines. In a)-d) intramolecular hydrogen bonds, O12–H12O···N11 and O22–H22O···N21, are highlighted by orange dashed lines.

Molecular and crystal structure of 2

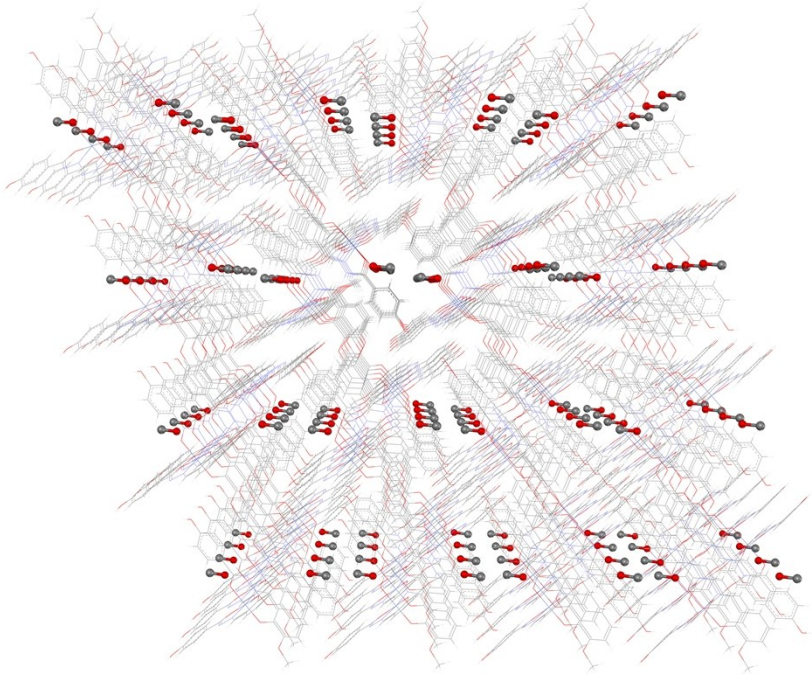

Fig. S15 Arrangement of guest methanol molecules present in the channels of the crystal structure viewed along the *a*-axis.

In the complex **2·0.7CH$_3$OH** the refinement of occupancy factors for the O1 and C1 methanol atoms gave value of 0.7. Due to that, the performance of data collection at 150(2) K is undertaken in order to confirm the presence of residual density in the crystal voids and it is also interpreted, but more reliably, as the 0.7 MeOH molecule per complex molecule. The final refinement procedure has been performed by PLATON SQUEEZE instruction at 296(2) K data.
Revealed by PARST and MERCURY programs the shortest intermolecular contacts between the methanol O1 atom and the complex molecule are formed with the methyl C215 atom and the five-membered hydrazone chelate ring O11 atom with the metrical values of O1···O11^{i} 3.69(2) Å (i=–x+1,–y+1,–z+2) for 296(2) K data and 3.12(2) Å for 150(2) K data and O1···C215^{ii} 3.44(2) Å (ii= x–1,+y,+z) for 296(2) K data and 3.19(2) Å for 150(2) K data. The O···O intermolecular distance of 3.69(2) Å is approx. 0.7 Å longer than the sum of van der Waals radii for an oxygen atom and its hardly be recognized as the O–H···O type of hydrogen bonding. Similarly, the O1···C215 contact at 296(2) K can be regarded as a very weak hydrogen bond of the C–H···O type due to weak acidity of C(sp^3)-H group.
It seems that all these contacts can be regarded, despite the geometrical criteria which are at the limiting values of the range, as supportive (especially C–H···O) as it is revealed by thermogravimetric analysis of the complex and capable to maintain methanol molecules accomodated in channels of complex molecules.

General and crystal data for 2·0.7MeOH: graphite–monochromated MoKα radiation (λ = 0.71073 Å), *a*=10.1424(6) Å, *b*=12.2350(10) Å, *c*=13.1652(8) Å, α=102.995(6)°, β=107.619(5) °, γ= 96.756(6) °, *V*=1486.54(18) Å^3, D_{calc}=1.449 g cm^{-3}, data / restraints / parameters= 6447/3/417, final *R* indices [$I>2\sigma(I)$]: R_1 = 0.0910; wR_2 = 0.1538, *R* indices (all data): R_1 = 0.1575; wR_2 = 0.1794 (see for comparison Table 5, compound **2** and CIF file for comprehensive data).

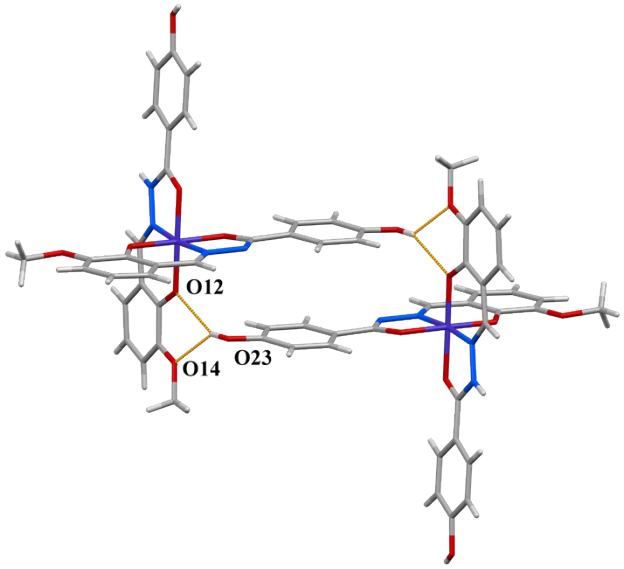

Fig. S16 Partial crystal structure of **2** showing formation of centrosymmetrical dimer *via* O23−H23O···O12 intermolecular hydrogen bond between hydroxyl group and the phenolate O12 donor atom. The H23O atom is bifurcated between O12 and O14 atoms as proton acceptors.

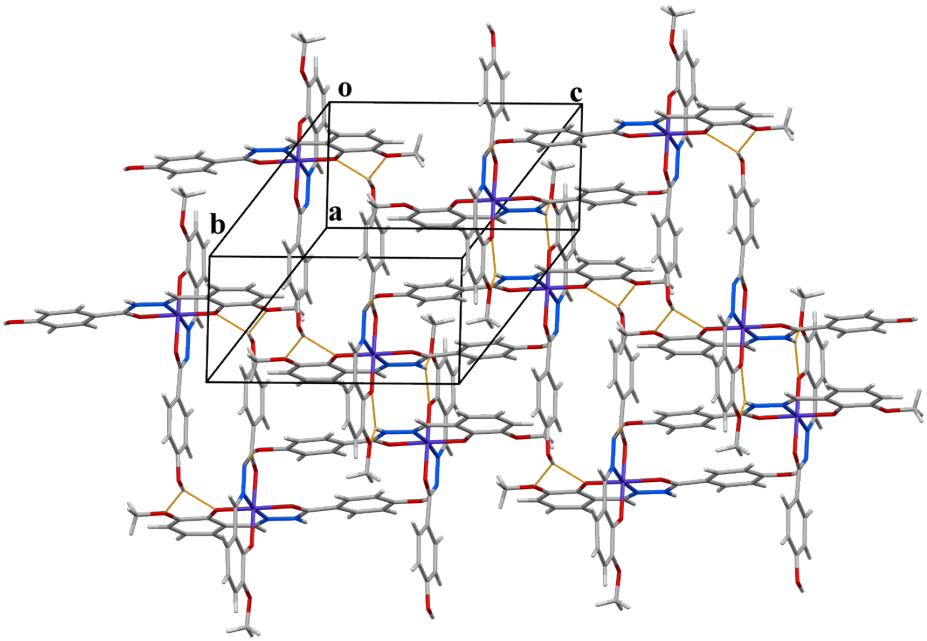

Fig. S17 Crystal structure of **2** showing 3D hydrogen-bonded supramolecular network

Molecular and crystal structure of 1 and 6

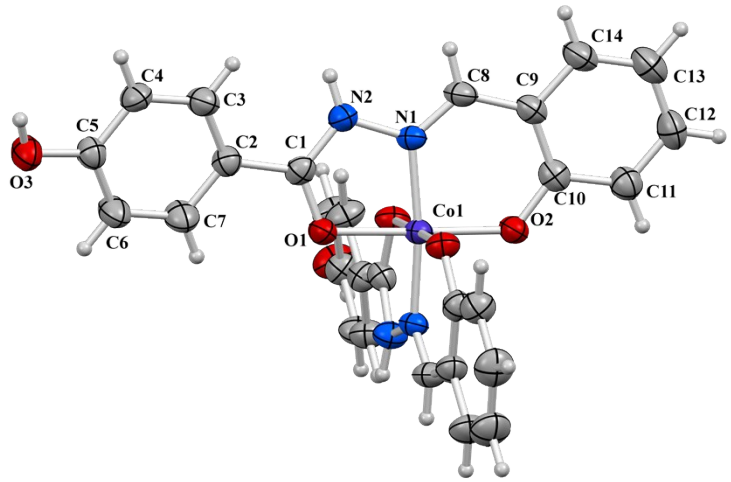

Fig. S18 Mercury–rendered ORTEP view of the molecular structure of complex **1**. The displacement ellipsoids are drawn at the 50% probability level at 296(2) K. The atom-numbering crystallographic scheme has been applied indicating asymmetric unit fragment. The hydrogen atoms are drawn as spheres of arbitrary radius.

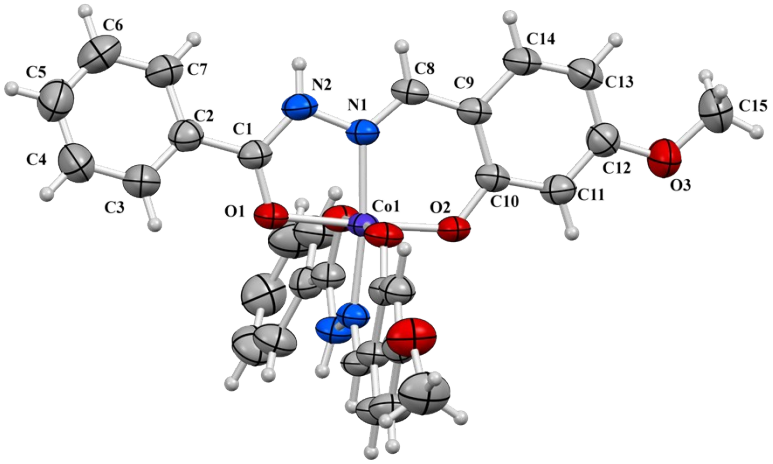

Fig. S19 Mercury–rendered ORTEP view of the molecular structure of complex **6·MeOH**. The displacement ellipsoids are drawn at the 50% probability level at 296(2) K. The atom-numbering crystallographic scheme has been applied. The hydrogen atoms are drawn as spheres of arbitrary radius. Methanol molecule has been omitted.

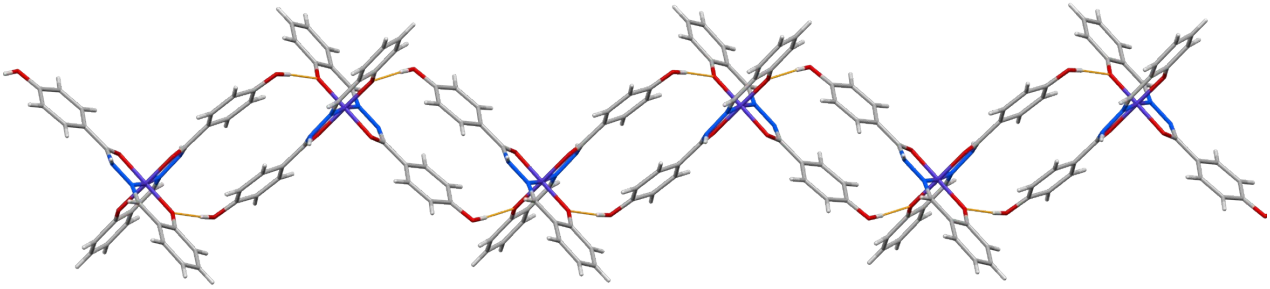

Fig. S20 Fraction of crystal structure of complex **1** showing assembling of complex molecules along *b* axis into 2D infinite chains of rings *via* O3−H13O···O2 intermolecular hydrogen bond.

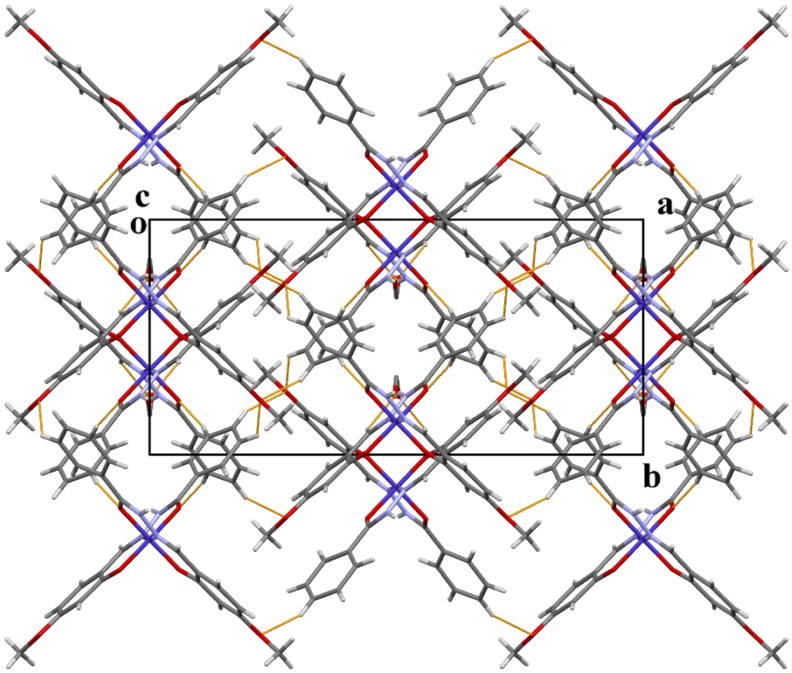

Fig. S21 Crystal packing of **6·MeOH** viewed in *ab* plane showing C−H···O intermolecular hydrogen bonds.

Selected bond lengths and angles

Table S1. Selected geometrical parameters for H_2L^3, H_2L^5 and H_2L^6 ligands.

A−B–C	***d*(A−B)/Å**	***d*(B–C)/Å**	**∠(A–B–C)/°**
H_2L^3			
O1–C1–C2	1.2285(14)	1.4816(16)	122.89(10)
O1–C1–N2	1.2285(14)	1.3508(14)	120.89(10)
C1–N2–N1	1.3508(14)	1.3757(14)	119.88(10)
N2–N1–C8	1.3757(14)	1.2777(14)	116.48(10)
N1–C8–C9	1.2777(14)	1.4455(16)	121.75(11)
C8–C9–C10	1.4455(16)	1.4067(16)	122.44(10)
C9–C10–O2	1.4067(16)	1.3597(14)	121.48(10)
H_2L^5			
O1–C1–C2	1.231(2)	1.495(2)	121.56(15)
O1–C1–N2	1.231(2)	1.348(2)	119.43(15)
C1–N2–N1	1.348(2)	1.3754(18)	122.16(14)
N2–N1–C8	1.3754(18)	1.276(2)	116.59(13)
N1–C8–C9	1.276(2)	1.449(2)	121.77(15)
C8–C9–C10	1.449(2)	1.399(2)	121.76(14)
C9–C10–O2	1.399(2)	1.3576(19)	122.97(15)
H_2L^6			
molecule 1			
O11–C11–C12	1.231(8)	1.510(9)	121.0(6)
O11–C11–N12	1.231(8)	1.319(8)	123.5(6)
C11–N12–N11	1.319(8)	1.374(7)	118.7(5)
N12–N11–C18	1.374(7)	1.283(7)	119.2(5)
N11–C18–C19	1.283(7)	1.452(8)	121.4(5)
C18–C19–C110	1.452(8)	1.407(8)	120.8(5)
C19–C110–O12	1.407(8)	1.337(8)	123.9(5)
molecule 2			
O21–C21–C22	1.230(6)	1.499(7)	122.3(4)
O21–C21–N22	1.230(6)	1.342(6)	122.0(4)
C21–N22–N21	1.342(6)	1.377(5)	119.2(4)
N22–N21–C28	1.377(5)	1.260(6)	118.1(4)
N21–C28–C29	1.260(6)	1.454(7)	120.5(5)
C28–C29–C210	1.454(7)	1.381(7)	122.4(4)
C29–C210–O22	1.381(7)	1.361(6)	122.2(5)

Table S2. Geometry of hydrogen bonds and C–H···O interactions (Å,°) for H_2L^3, H_2L^5 and H_2L^6 ligands.

D–H···A	D–H	H···A	D···A	∠D–H···A	Symmetry code
			H_2L^3		
O2–H2O···N1	0.842(16)	1.884(15)	2.6322(14)	147.3(15)	–
N2–H2N···O2	0.863(14)	2.383(13)	3.1241(14)	144.2(12)	x,1/2–y,1/2+z
O3–H3O···O1	0.862(16)	1.833(16)	2.6873(12)	171.1(16)	1–x,1/2+y,1/2–z
C3–H3···O3	0.9300	2.571(1)	3.249(2)	130.09(8)	x,3/2–y,–1/2+z
C15–H15B···O1	0.9600	2.559(1)	3.304(2)	134.57(10)	–x,–1/2+y,–1/2–z
			H_2L^5		
O2–H2O···N1	0.843(18)	1.874(18)	2.6391(17)	150.3(17)	–
N2–H2N···O1	0.891(16)	1.974(17)	2.8622(18)	174.6(17)	1–x,1–y,–z
C5–H5···O3	0.9300	2.468(1)	3.393(2)	173.25(12)	3/2–x,–1/2+y,1/2–z
C7–H7···O2	0.9300	2.652(1)	3.435(2)	142.22(11)	x,–1+y,z
			H_2L^6		
O12–H12O···N11	0.85(6)	1.85(7)	2.629(7)	153(7)	–
O22–H22O···N21	0.82(5)	1.85(6)	2.604(6)	153(6)	–
N12–H12N···O11	0.88(5)	2.13(4)	2.988(7)	166(5)	x,–y,–1/2+z
N22–H22N···O21	0.88(4)	1.99(4)	2.817(5)	156(4)	x,1–y,–1/2+z
C26 —H26···O11	0.9300	2.593(5)	3.499(9)	164.54(45)	–1+x,–y,–1/2+z
C28 –H28···O21	0.9300	2.569(3)	3.312(6)	137.22(33)	x,1–y,–1/2+z
C114–H114···O22	0.9300	2.472(4)	3.296(7)	147.60(37)	x,1–y,–1/2+z
C17 –H17···O11	0.9300	2.634(4)	3.334(7)	132.57(42)	x,–y,–1/2+z

Table S3(a). Selected bond lengths [Å] and angles [°] for **2**.

Complex	**2**
Co(1)–N(11)	1.880(2)
Co(1)–N(21)	1.867(2)
Co(1)–O(12)	1.879(2)
Co(1)–O(22)	1.899(2)
Co(1)–O(11)	1.928(2)
Co(1)–O(21)	1.884(2)
O(11)–C(11), O(21)–C(21)	1.278(3); 1.309(3)
O(12)–C(110), O(22)–C(210)	1.316(4); 1.325(3)
N(11)–C(18), N(21)–C(28)	1.287(4) ; 1.283(4)
N(11)–N(12), N(21)–N(22)	1.380(3); 1.385(3)
N(12)–C(11), N(22)–C(21)	1.333(4); 1.315(4)
Bond angles	
N(21)–Co(1)–O(12)	90.40(10)
N(21)–Co(1)–N(11)	171.65(10)
O(12)–Co(1)–N(11)	94.87(10)
N(21)–Co(1)–O(21)	83.18(10)
O(12)–Co(1)–O(21)	91.09(10)
N(11)–Co(1)–O(21)	90.22(10)
N(21)–Co(1)–O(22)	96.14(10)
O(12)–Co(1)–O(22)	89.96(10)
N(11)–Co(1)–O(22)	90.36(9)
O(21)–Co(1)–O(22)	178.75(9)
N(21)–Co(1)–O(11)	91.28(10)
O(12)–Co(1)–O(11)	177.53(9)
N(11)–Co(1)–O(11)	83.27(10)
O(21)–Co(1)–O(11)	87.31(9)
O(22)–Co(1)–O(11)	91.66(9)

Table S3(b). Selected bond lengths [Å] and angles [°] for **1** and **6**·MeOH.

Complex	**1**	**6**·MeOH
Co(1)–N(1)^{i,ii}	1.874(3)	1.876(2)
Co(1)–N(1)	1.874(3)	1.876(2)
Co(1)–O(2)	1.884(2)	1.886(2)
Co(1)–O(2)^{i,ii}	1.884(2)	1.886(2)
Co(1)–O(1)^{i,ii}	1.892(2)	1.921(2)
Co(1)–O(1)	1.892(2)	1.921(2)
O(1)–C(1)	1.289(4)	1.285(3)
O(2)–C(10)	1.324(4)	1.313(3)
N(1)–C(8)	1.282(4)	1.273(4)
N(1)–N(2)	1.403(4)	1.405(3)
N(2)–C(1)	1.325(4)	1.331(4)
Bond angles		
N(1)^{i,ii}–Co(1)–N(1)	172.05(18)	172.48(15)
N(1)^{i,ii}–Co(1)–O(2)	90.36(11)	91.27(9)
N(1)–Co(1)–O(2)	95.24(11)	94.06(9)
N(1)^{i,ii}–Co(1)–O(2)^{i,ii}	95.24(11)	94.06(9)
N(1)–Co(1)–O(2)^{i,ii}	90.36(11)	91.27(9)
O(2)–Co(1)–O(2)^{i,ii}	90.41(15)	89.73(14)
N(1)^{i,ii}–Co(1)–O(1)^{i,ii}	83.68(11)	83.24(9)
N(1)–Co(1)–O(1)	83.68(11)	83.24(9)
N(1)–Co(1)–O(1)^{i,ii}	90.64(11)	91.40(9)
O(2)–Co(1)–O(1)^{i,ii}	90.33(10)	90.60(9)
O(2)^{i,ii}–Co(1)–O(1)	90.33(10)	90.61(9)
O(2)^{i,ii}–Co(1)–O(1)^{i,ii}	178.70(10)	177.28(8)
O(2) –Co(1)–O(1)	178.70(10)	177.28(8)
N(1)^{i,ii}–Co(1)–O(1)	90.64(11)	91.40(9)
O(1)^{i,ii}–Co(1)–O(1)	88.95(15)	89.18(13)

Symmetry transformations used to generate equivalent atoms: i = –x, –y+1/2, z for **1** and ii = –x+1,y,–z+3/2 for **6**·MeOH

Table S4. Hydrogen bonds for **1**, **2** and **6**·MeOH [Å and °].

D–H···A	d(D–H)	d(H···A)	d(D···A)	<(DHA)	Symmetry code
1					
O3–H13O···O2	0.83(3)	1.86(3)	2.685(4)	175(3)	x,+y−1/2, −z
O3–H13O···N1	0.83(3)	2.84(4)	3.209(4)	110(3)	−x, −y, −z
N2–H12N···N2	0.86(5)	1.98(5)	2.810(4)	162(4)	−x−1/2,+y, −z
C4–H4···O2	0.93	2.76	3.373(4)	124	x,+y−1/2, −z
C11–H11···O3	0.93	2.76	3.416(5)	128	x,+y+1/2, −z
C12–H12···O3	0.93	2.60	3.399(5)	144	x−1/2,+y+1/2,+z+1/2
2					
O23–H23O···O12	0.82(3)	2.25(4)	2.988(3)	149(3)	−x+2, −y+1, −z+2
O23–H23O···O14	0.82(3)	2.08(3)	2.749(4)	139(3)	−x+2, −y+1, −z+2
O13–H13O···N22	0.82(4)	1.94(4)	2.734(4)	163(4)	−x+1, −y+1, −z+1
O13 –H13O···N21	0.82(4)	2.80(4)	3.441(4)	137(3)	−x+1, −y+1, −z+1
N12–H12N···O22	0.84(3)	2.40(3)	3.069(3)	137(3)	−x+1, −y, −z+1
N12–H12N···O24	0.84(3)	2.10(4)	2.778(4)	138(3)	−x+1, −y, −z+1
C18–H18···O22	0.93	2.62	3.339(4)	134	−x+1, −y, −z+1
C18–H18···O24	0.93	2.66	3.287(5)	125	−x+1, −y, −z+1
C13–H13···O24	0.93	2.76	3.573(5)	147	−x+1, −y, −z+1
C14–H14···O23	0.93	2.64	3.364(6)	135	−x+2, −y+1, −z+1
C28–H28···O13	0.93	2.82	3.377(4)	120	−x+1, −y+1, −z+1
C16–H16···N22	0.93	2.76	3.417(5)	129	−x+1, −y+1, −z+1
C23–H23···O13	0.93	2.93	3.674(5)	138	−x+1, −y, −z+2
C24–H24···O12	0.93	2.91	3.541(3)	127	−x, −y, −z+1
6·MeOH					
N2 –H12N ···O4	0.86(5)	1.94 (4)	2.763(5)	161(4)	−x+1, −y+2, −z+1
C7–H7···O4	0.93	2.73	3.538(6)	145	−x+1, −y+2, −z+1
C8–H8···O4	0.93	2.54	3.303(5)	139	−x+1, −y+2, −z+1
C4–H4···O3	0.93	2.51	3.183(5)	129	−x+1,+y−1, −z+1/2+1
C5–H5···O3	0.93	2.68	3.508(5)	149	x−1/2, −y+1/2+1,+z−1/2
C6–H6···O1	0.93	2.58	3.496(5)	169	x, −y+1,+z−1/2
C8–H8···O2	0.93	2.80	3.587(3)	144	x, −y+2,+z−1/2
C14–H14···O2	0.93	2.81	3.600(3)	144	x, −y+2,+z−1/2

NMR spectroscopy

R = OH, R'= H, R" = H	**1**
R = OH, R'= H, R" = OCH_3	**2**
R = OH, R'= OCH_3, R" = H	**3**
R = H, R'= H, R" = H	**4**
R = H, R'= H, R" = OCH_3	**5**
R = H, R' = OCH_3, R" = H	**6**

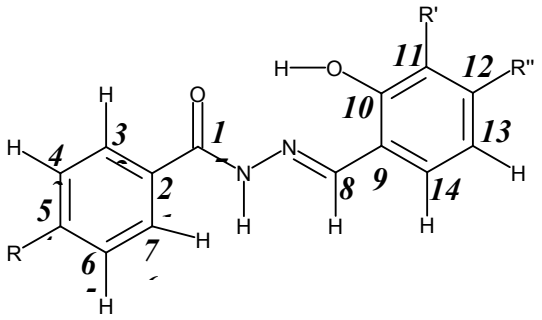

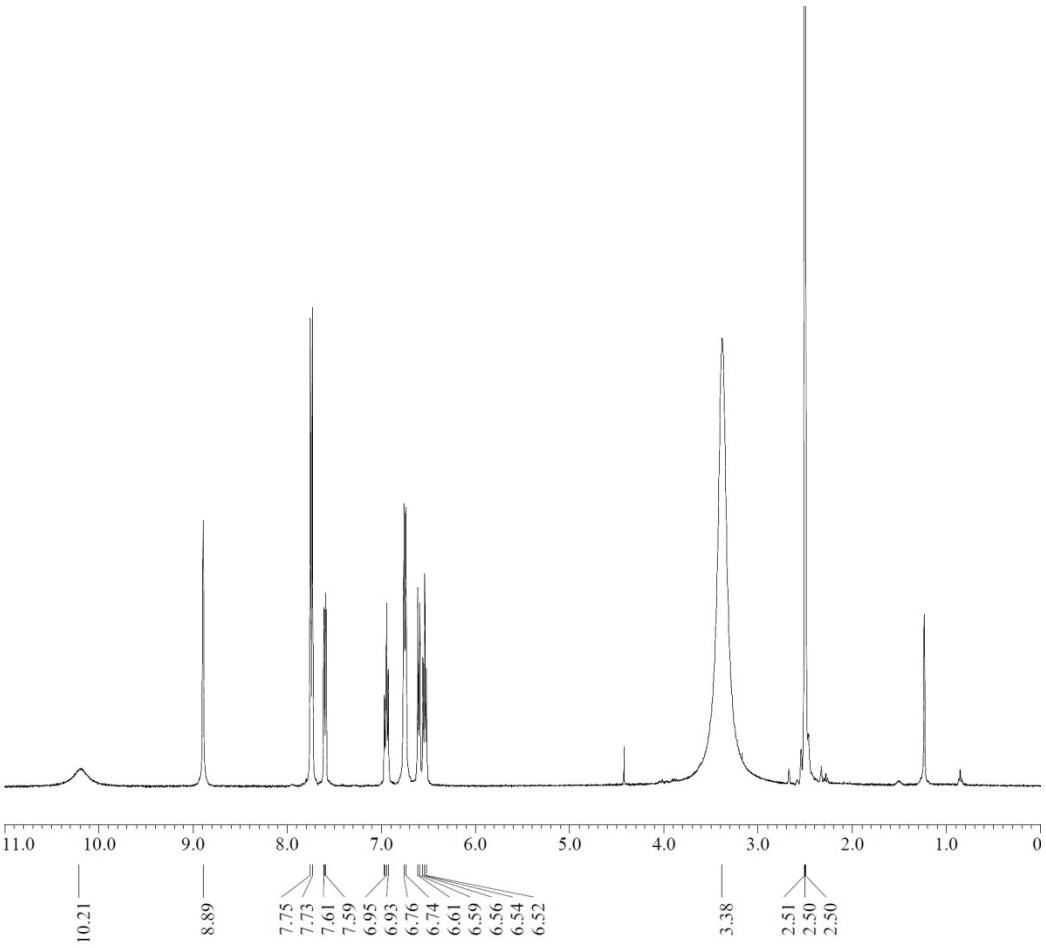

Fig. S22 ^{1}H NMR spectrum of **[**Co(HL^1)(L^1)] in DMSO-d_6.

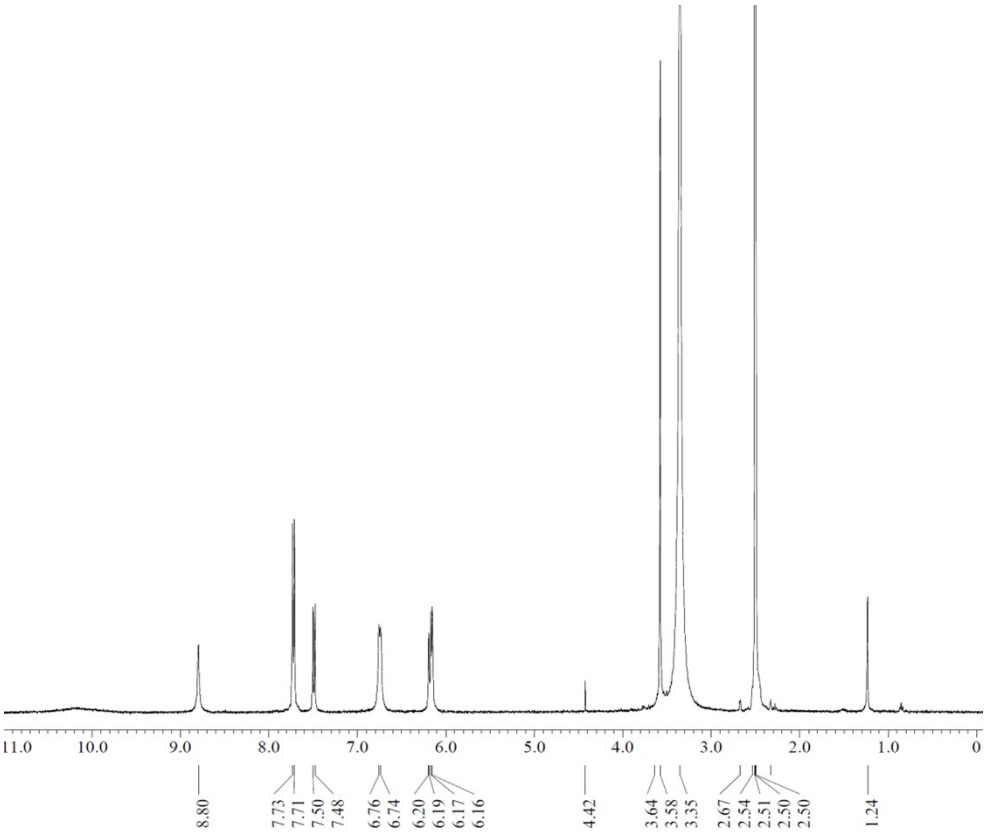

Fig. S23 ^{1}H NMR spectrum of [Co(HL^{2})(L^{2})] in DMSO-d_6.

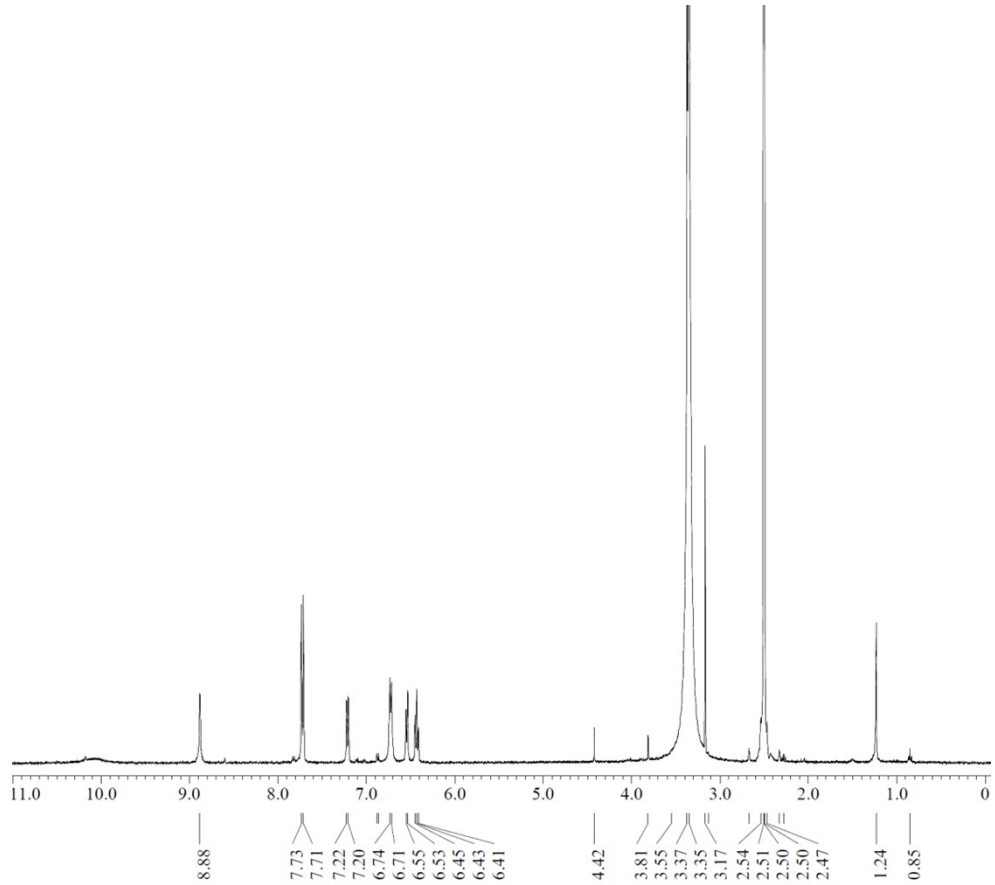

Fig. S24 ^{1}H NMR spectrum of [Co(HL^{3})(L^{3})] in DMSO-d_6.

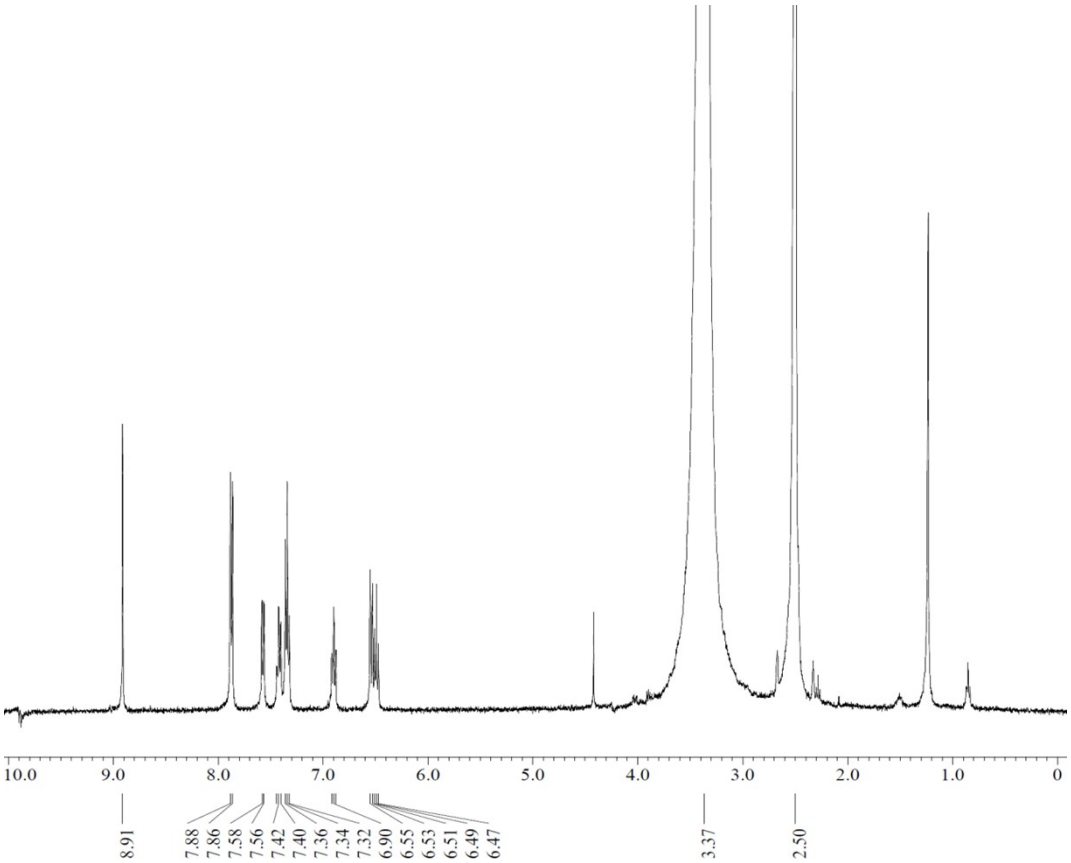

Fig. S25 ^{1}H NMR spectrum of [Co(HL^{4})(L^{4})] (4) in DMSO-d_6.

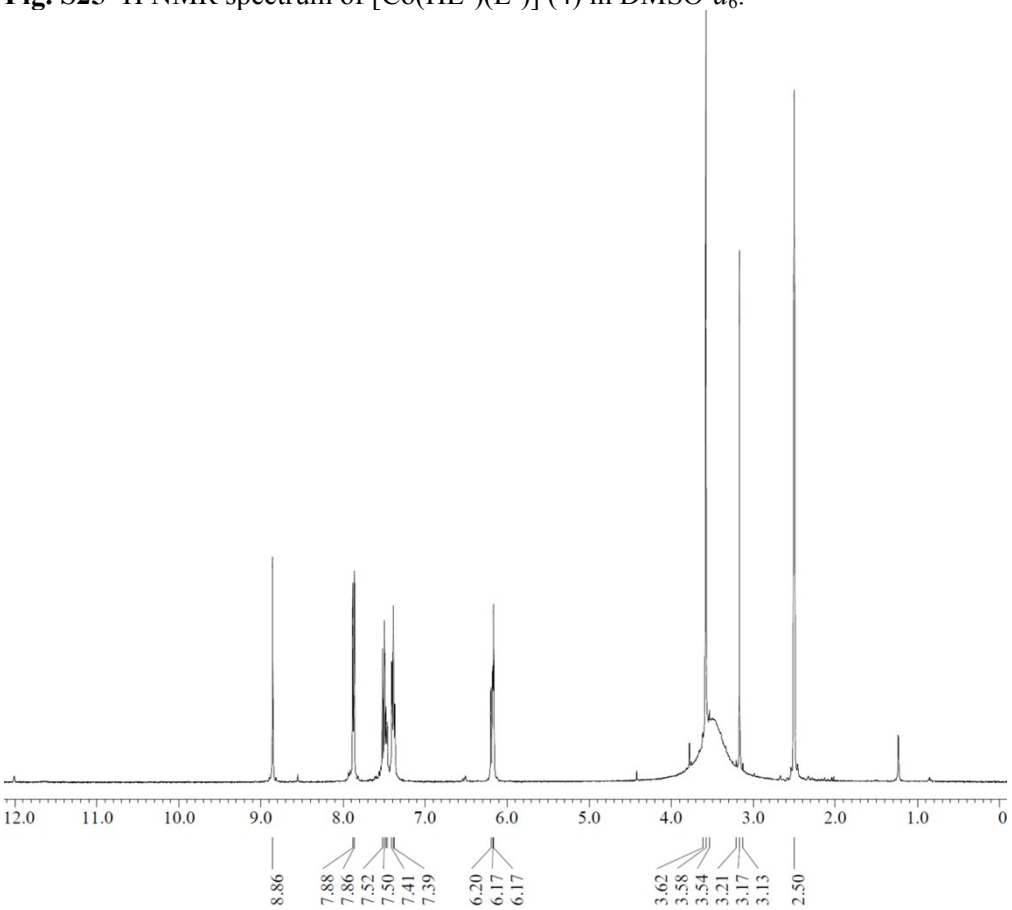

Fig. S26 ^{1}H NMR spectrum of [Co(HL^{5})(L^{5})] in DMSO-d_6.

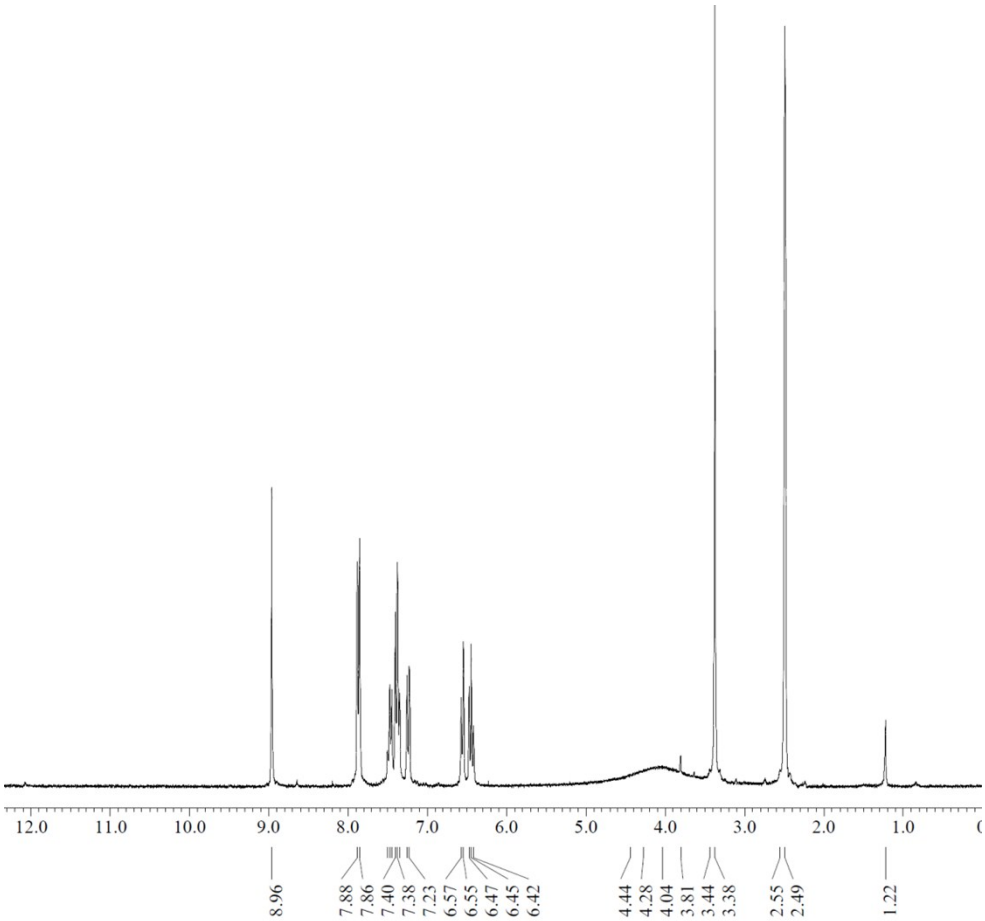

Fig. S27 ^{1}H NMR spectrum of [Co(HL^{6})(L^{7})] in DMSO-d_6.

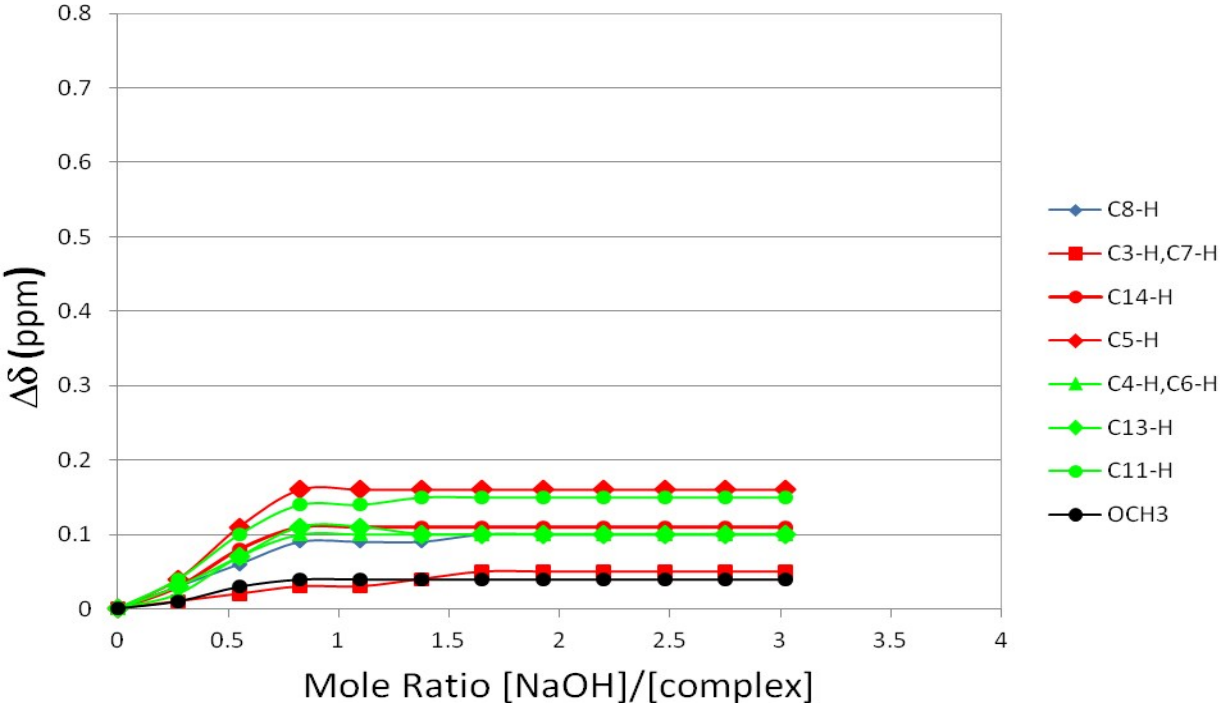

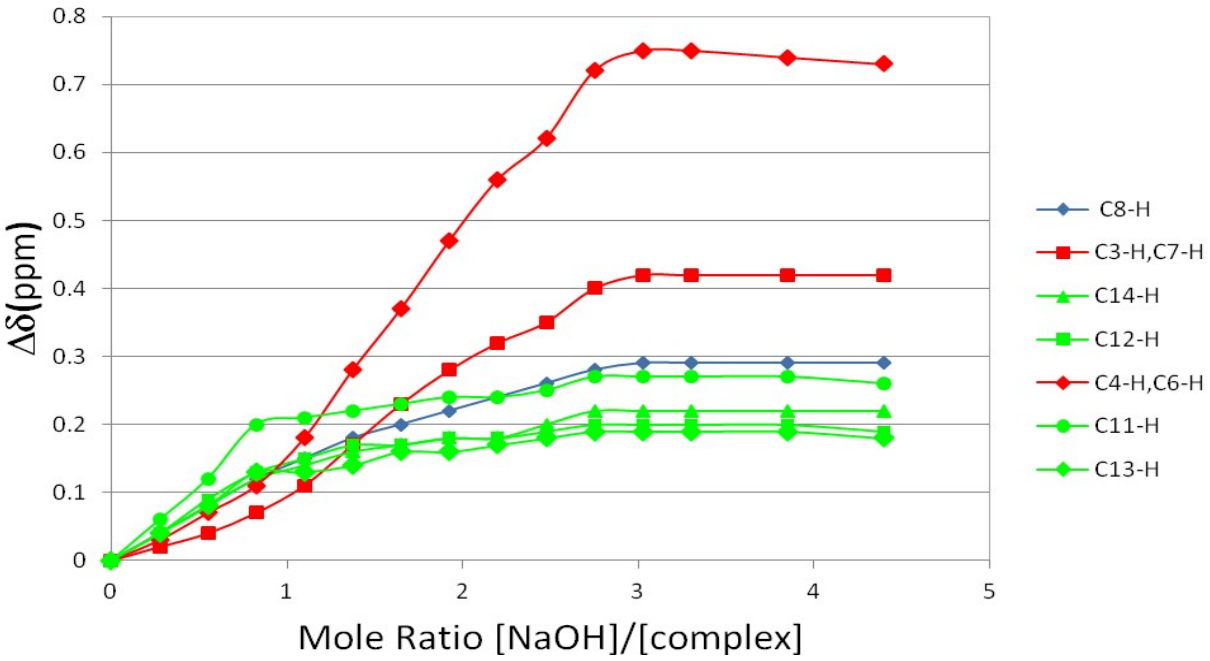

Fig. S28 (a) ^{1}H NMR Δδ (ppm) of the signals of [Co(HL^{5})(L^{5})] at various [NaOH]/[complex] ratios; (b) ^{1}H NMR Δδ (ppm) of the signals of [Co(HL^{1})(L^{1})] at various [NaOH]/[complex] ratios.

(a)

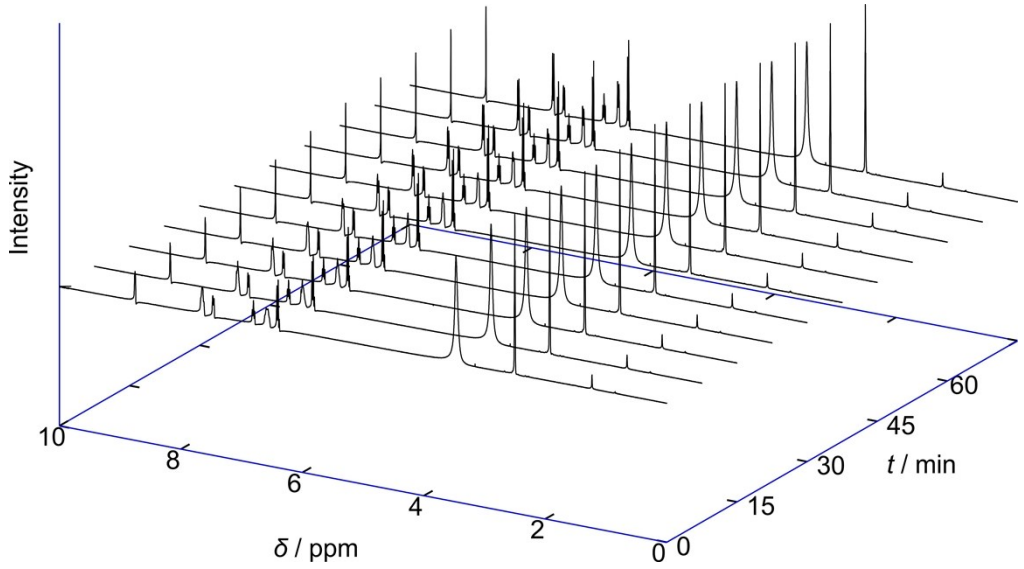

(b)

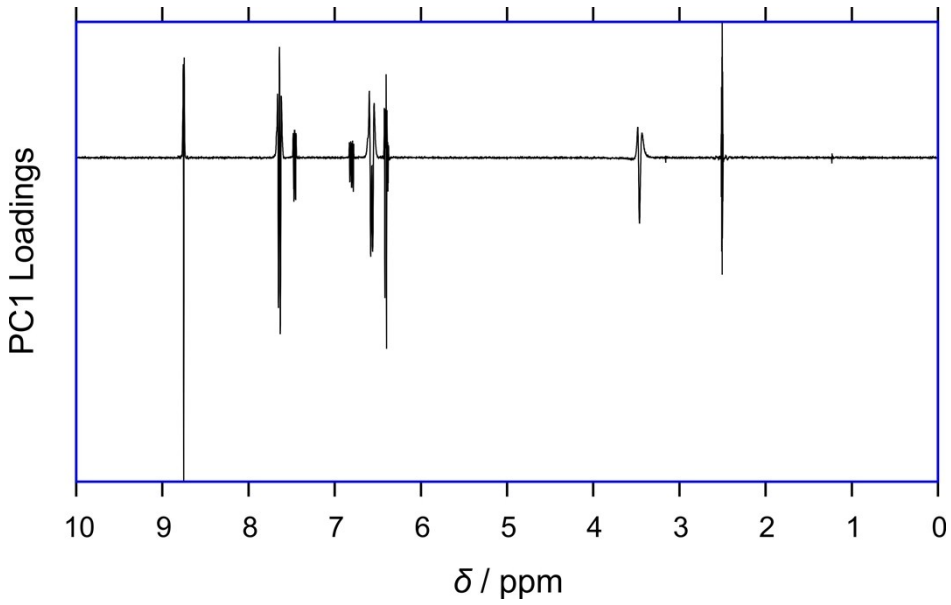

Fig. S29 (a) ^{1}H NMR spectrum of complex **1** in DMSO-d_6 with a ratio [NaOH] /[complex] = 1.1 recorded in dependence of time. (b) PC1 loadings obtained by principal component analysis of NMR spectra presented on Fig. 29a.